Deep excursion beyond the proton dripline. II. Toward the limits of existence of nuclear structure

L. V. Grigorenko,[1,2,3] I. Mukha,[4] D. Kostyleva,[5,4,*] C. Scheidenberger,[4,5] L. Acosta,[6,7] E. Casarejos,[8] V. Chudoba,[1,9] A. A. Ciemny,[10] W. Dominik,[10] J. A. Dueñas,[11] V. Dunin,[12] J. M. Espino,[13] A. Estradé,[14] F. Farinon,[4] A. Fomichev,[1] H. Geissel,[4,5] A. Gorshkov,[1] Z. Janas,[10] G. Kamiński,[15,1] O. Kiselev,[4] R. Knöbel,[4,5] S. Krupko,[1] M. Kuich,[16,10] Yu. A. Litvinov,[4] G. Marquinez-Durán,[17] I. Martel,[17] C. Mazzocchi,[10] E. Yu. Nikolskii,[3,1] C. Nociforo,[4] A. K. Ordúz,[17] M. Pfützner,[10,4] S. Pietri,[4] M. Pomorski,[10] A. Prochazka,[4] S. Rymzhanova,[1] A. M. Sánchez-Benítez,[18] P. Sharov,[1] H. Simon,[4] B. Sitar,[19] R. Slepnev,[1] M. Stanoiu,[20] P. Strmen,[19] I. Szarka,[19] M. Takechi,[4] Y. K. Tanaka,[4,21] H. Weick,[4] M. Winkler,[4] J. S. Winfield,[4] X. Xu,[22,5,4] and M. V. Zhukov[23]

[1]*Flerov Laboratory of Nuclear Reactions, JINR, 141980 Dubna, Russia*
[2]*National Research Nuclear University MEPhI, 115409 Moscow, Russia*
[3]*National Research Centre, Kurchatov Institute, Kurchatov Square 1, 123182 Moscow, Russia*
[4]*GSI Helmholtzzentrum für Schwerionenforschung GmbH, 64291 Darmstadt, Germany*
[5]*II. Physikalisches Institut, Justus-Liebig-Universität, 35392 Gießen, Germany*
[6]*INFN, Laboratori Nazionali del Sud, Via Santa Sofía, 95123 Catania, Italy*
[7]*Instituto de Física, Universidad Nacional Autónoma de México, México, Distrito Federal 01000, Mexico*
[8]*University of Vigo, 36310 Vigo, Spain*
[9]*Institute of Physics, Silesian University Opava, 74601 Opava, Czech Republic*
[10]*Faculty of Physics, University of Warsaw, 02-093 Warszawa, Poland*
[11]*Departamento de Ingenieria Electrica y Centro de Estudios Avanzados en Fisica, Matemáticas y Computación, Universidad de Huelva, 21071 Huelva, Spain*
[12]*Veksler and Baldin Laboratory of High Energy Physics, JINR, 141980 Dubna, Russia*
[13]*Department of Atomic, Molecular and Nuclear Physics, University of Seville, 41012 Seville, Spain*
[14]*University of Edinburgh, EH1 1HT Edinburgh, United Kingdom*
[15]*Heavy Ion Laboratory, University of Warsaw, 02-093 Warszawa, Poland*
[16]*Faculty of Physics, Warsaw University of Technology, 00-662 Warszawa, Poland*
[17]*Department of Applied Physics, University of Huelva, 21071 Huelva, Spain*
[18]*Centro de Estudios Avanzados en Física, Matemáticas y Computación (CEAFMC), Department of Integrated Sciences, University of Huelva, 21071 Huelva, Spain*
[19]*Faculty of Mathematics and Physics, Comenius University, 84248 Bratislava, Slovakia*
[20]*IFIN-HH, Post Office Box MG-6, Bucharest, Romania*
[21]*University of Tokyo, 113-0033 Tokyo, Japan*
[22]*School of Physics and Nuclear Energy Engineering, Beihang University, 100191 Beijing, China*
[23]*Department of Physics, Chalmers University of Technology, S-41296 Göteborg, Sweden*

(Received 19 June 2018; revised manuscript received 6 September 2018; published 7 December 2018)

Prospects of experimental studies of argon and chlorine isotopes located far beyond the proton dripline are studied by using systematics and cluster models. The deviations from the widespread systematics observed in ^{28,29}Cl and ^{29,30}Ar have been theoretically substantiated, and analogous deviations have been predicted for the lighter chlorine and argon isotopes. The limits of nuclear structure existence are predicted for Ar and Cl isotopic chains, with ^{26}Ar and ^{25}Cl found to be the lightest sufficiently long-living nuclear systems. By simultaneous measurements of protons and γ rays following decays of such systems as well as their β-delayed emission, an interesting synergy effect may be achieved, which is demonstrated by the example of ^{30}Cl and ^{31}Ar ground-state studies. Such a synergy effect may be provided by the new EXPERT setup (EXotic Particle Emission and Radioactivity by Tracking) being operated inside the fragment separator and spectrometer facility at GSI, Darmstadt.

DOI: 10.1103/PhysRevC.98.064309

I. INTRODUCTION

Several states in proton (p)-unbound isotopes ^{28}Cl, ^{30}Cl, and ^{29}Ar were reported recently [1]. This work continues the research published in Refs. [1–4]. The systematics and cluster model studies in Ref. [1] allowed us to interpret the data as observations of the ground state (g.s.) in ^{28}Cl, the g.s. and three excited states in ^{30}Cl, and one state in ^{29}Ar (either the ground state or an excited state). Also the reported spectrum of ^{31}Ar allowed for prescription of the g.s. energy

*Corresponding author: D.Kostyleva@gsi.de

of this isotope by using the isobaric symmetry systematics. Together with the known p-unbound isotopes ^{14,15,16}F, the studied argon and chlorine isotopes constitute the most deeply studied particle-unstable isotopic chains in the whole $Z \leqslant 20$ nuclei region.

In this work we continue the "excursion beyond the proton dripline" of Ref. [1]. We intend to answer the question: What impact does the obtained experimental results have on our understanding of prospects to study the other nuclides located far (e.g., 2–5 mass units) beyond the driplines? Correspondingly, we discuss the following three main topics.

(i) The previously published systematics of one-proton ($1p$) separation energies [1] are extrapolated further into the unexplored region beyond the proton dripline. The obtained results for the experimentally observed cases ($^{28-30}$Cl nuclides) are considerably different from the systematic trends available in the literature [5–7]. We extrapolate this systematics to the lightest chlorine and argon isotopes in Sec. III. The smaller than expected values of the decay energies suggest longer-living states and, consequently, weaker limitations on the nuclear-structure existence beyond the dripline.

(ii) We clarify the prospects of a limit of the nuclear structure existence by using the obtained information on the separation energies. We assume that a nuclear configuration has an individual structure with at least one distinctive state, if the orbiting valence protons of the system are reflected from the corresponding nuclear barrier at least one time. Thus nuclear half-life may be used as a gauge of such a limit. It is clear that the very long-lived particle-emitting states are *quasistationary*. This means that they can be considered as *stationary for the majority of practical applications*. For example, the half-lives of all known heavy two-proton ($2p$) radioactivity cases (^{45}Fe, ^{48}Ni, and ^{54}Zn) are a few milliseconds. Thus, their $2p$ decays are so slow that weak transitions become their competitors with branching ratio of dozens of percent [8]. We may assume that modification of the nuclear structure by continuum coupling is absolutely negligible for such states. In contrast, the continuum coupling becomes increasingly important for broad ground states beyond the driplines. For example, see the discussion connected with studies of the ^{10}He g.s. in Ref. [9]. This work demonstrated that the observed continuum properties of ^{10}He can be crucially modified by peculiarities of the initial nuclear structure of the reaction participants for the widespread experimental approaches (e.g., knockout reactions). Such a situation can be regarded as transitional to *continuum dynamics*, where the observable continuum response is also defined by the reaction mechanism and the initial nuclear structure. Here the properties, interpretable as the nuclear structure of the reaction products, cannot be reliably extracted from the measured data. For example, we may refer to the well-known tetra-neutron system in continuum [10], where such an ambiguity has been demonstrated by applying the realistic scenario of the tetraneutron population. Within the topic of the above discussion, we predict the limits of nuclear-structure existence to be near the ^{25}Cl and ^{26}Ar isotopes in Sec. IV.

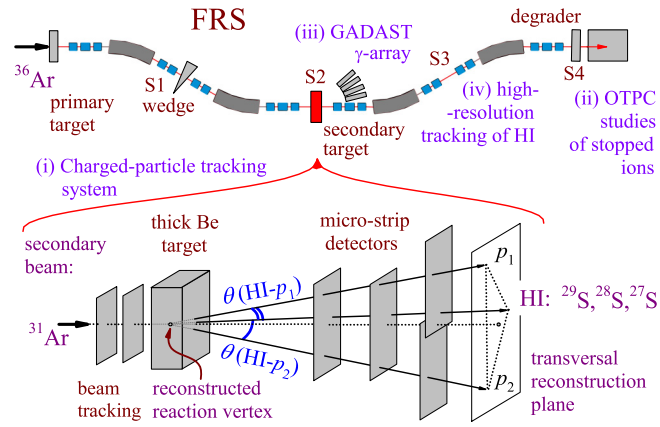

FIG. 1. The EXPERT pilot setup installed in the FRS. (i) Charged-particle tracking system shown in the lower inset consisted of beam-tracking Si detectors providing energy loss and timing information and microstrip Si detectors for precise tracking of the decay products of nuclei of interest. (ii) Optical time projection chamber (OTPC) for detection of radioactivity in the millisecond range. (iii) Array of γ-ray detectors around the secondary target, GADAST. (iv) Detectors for identification of heavy ions and precise measurements of their momenta.

(iii) The experimental setup, used in Refs. [1–4], is a pilot version of the EXPERT (EXotic Particle Emission and Radioactivity by Tracking) setup planned by the Super-FRS Experiment Collaboration of the FAIR project (see Refs. [11,12] and Fig. 1). The tracking system for light ions and the γ-ray detector were installed downstream of the secondary target in the internal focal plane of the fragment separator FRS at GSI, Darmstadt (see the details in Ref. [1]). The first half of the FRS was set for production and separation of ^{31}Ar ions, and the second half was used as a spectrometer for heavy-ion decay products. The optical time projection chamber (OTPC) installed at S4 was studying β-delayed particle emission and radioactive decays of heavy fragments living long enough to pass through the 30 m of the S2–S4 second half of the FRS. In this article we demonstrate that the complementary measurements performed by all components of the EXPERT setup can be combined together, which allows for the synergy effect in studies of the abovementioned unbound nuclear systems. Such an effect is demonstrated in Sec. V by examples of ^{30}Cl and ^{31}Ar studies.

II. THE THEORETICAL MODELS APPLIED

We apply several simple theoretical tools in this work. The systematics of $1p$-separation energies S_p in chlorine isotopes are studied by using the core + p potential cluster model from

Ref. [1]. The systematics of Coulomb displacement energies in such a model is sensitive to two basic parameters: (i) an orbital size (governed by a potential radius) and (ii) the charge radius of the core. These parameters are varied in the model in a systematic way.

The systematics of $2p$-separation energies S_{2p} in argon isotopes are based on (i) the S_p values obtained from the systematics of the related chlorine isotopes and (ii) the systematics of odd-even staggering energies based on the corresponding long isotopic and isotonic chains. This approach was actively used in our previous works [1,2], and it has proven to be a very reliable tool with easily estimated uncertainties.

The $1p$-decay widths of chlorine isotopes are calculated by using the abovementioned potential cluster model. We assume that the internal normalization of continuum states is an indicator of their resonance behavior. Such an indicator is more tractable for the broad states in comparison with the corresponding behavior of the phase shifts. We also use the R-matrix model for the $1p$-decay width estimates in the case of very narrow states.

The three-body $2p$-decay widths of argon isotopes are estimated by using the R-matrix-type model from Ref. [8]. This model can be traced back to the three-body approximation with a simplified three-body Hamiltonian, which neglects nucleon-nucleon interaction [13,14]. The widths calculated by this model match the corresponding calculations of the complete three-body model within a factor of 10 in the worst case. In the specific case of $2p$-decay width estimates of ^{26}Ar, we use the sophisticated three-body core $+ 2p$ cluster model developed for its mirror isobaric partner ^{26}O in Refs. [15,16].

The unit system $\hbar = c = 1$ is used in this work.

III. CHLORINE AND ARGON ISOTOPIC CHAINS FAR BEYOND THE PROTON DRIPLINE

The isotopes between ^{32}Cl and ^{28}Cl have been studied in Ref. [1] by applying the two-body cluster ^{A}S $+ p$ model. The major parameters of the model (potential and charge radii of the sulfur core nucleus) were systematically varied (see Table I in Ref. [1]). The Thomas-Ehrman effect [17,18], especially pronounced in the sd-shell nuclei, is well accounted for by such a model. As a result, a consistent description of the known low-lying spectra of ^{32}Cl and ^{31}Cl was obtained as well as a reasonable explanation of the newly observed states in the ^{30}Cl, ^{29}Cl, and ^{28}Cl nuclei.

Here we estimate the further isotopes beyond the proton dripline: $^{25-27}$Cl and $^{26-28}$Ar. The problem here is that for the lighter chlorine isotopes, the respective "core nuclei" $^{24-26}$S are particle unbound with the separation energies estimated in Table I. These estimates are partly illustrated in Fig. 2. So, the main decay channels are expected to be $2p$, $3p$, and $4p$ emission from ^{26}S, ^{25}S, and ^{24}S, respectively. One may notice that the decay energies of various decay branches of sulfur isotopes are much smaller than those of $1p$ emission from chlorine or $2p$ emission from argon isotopes. This means that the decay mechanism of $^{25-27}$Cl should be sequential emission of one proton followed by emission of two to four protons from the respective sulfur daughter. Similarly, the decay mechanism of $^{26-28}$Ar should be sequential emission of two protons followed by emission of two to four protons. The half-life values of such sequential decays are practically entirely defined by the first "fast" step of sequential proton emission with large Q_{2p} value. Therefore we do not take into account the particle instability of $^{24-26}$S in the following half-life estimates.

TABLE I. Estimated two-proton S_{2p}, three-proton S_{3p}, and four-proton S_{4p} separation energies in MeV for three sulfur isotopes beyond the proton dripline.

Isotope	S_{2p}	S_{3p}	S_{4p}
^{26}S	− 1.3	2.0	2.1
^{25}S	− 3.0	− 5.3	− 3.5
^{24}S	− 6.0	− 8.1	− 5.4

The results of the cluster ^{A}S $+ p$ model calculations from Ref. [1] for ^{26}Cl and ^{27}Cl are shown in Fig. 3. For the calculation of ^{25}Cl we used the ^{24}O $+ n$ potential developed for studies of ^{26}O in Ref. [16]. The ^{25}O spectrum is quite "poor": it contains just one known d-wave $3/2^+$ state [19–21]. By adding Coulomb interaction to the potential we obtain the ^{25}Cl g.s. at $E_r = -S_p = 6.0$–6.3 MeV. The E_r uncertainty here is defined by the ^{24}S "charge radius" uncertainty taken in accordance with Fig. 12 of Ref. [1].

The systematics of proton separation energies S_p for the chlorine isotopic chain is given in Fig. 5(a). For illustration purposes we use here the data compiled in the National Nuclear Data Center database [5], the standard AME2012 evaluation [6], and the recent isobaric multiplet mass evaluation [7]. One may see that the predicted systematics of Ref. [7] along the isobaric chain exactly follows the experimentally known systematics along the isotonic chain and can be regarded as trivial, while the predictions of Ref. [6] somewhat deviate from the isotone evolution. The predictions of our cluster model here and in Ref. [1] (where they are supported by

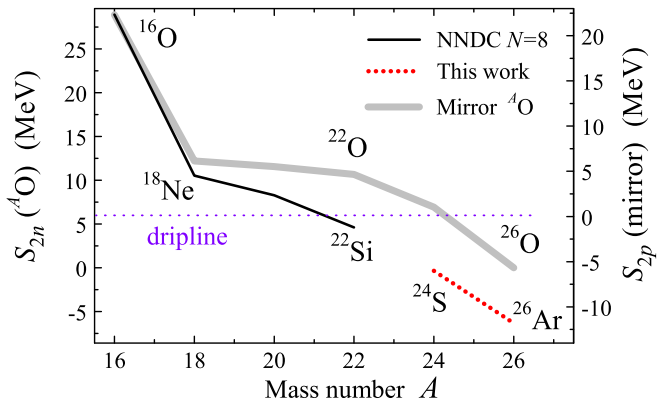

FIG. 2. The S_{2p} estimates for ^{24}S (see also Table I). Two-neutron separation energies S_{2n} for the oxygen isotopic chain from Ref. [5] are shown by the thick gray line, and two-proton separation energies S_{2p} for the mirror isotope chains are shown by the solid black line. The red dotted line corresponds to the calculated S_{2p} value for ^{26}Ar (see Sec. IV and Fig. 6) and the linear interpolation for ^{24}S.

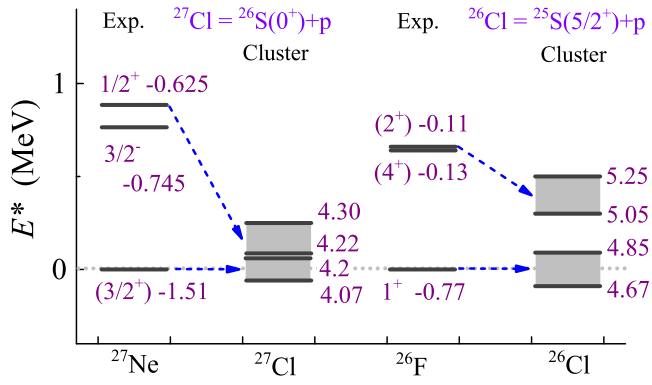

FIG. 3. Energy levels of ^{26}Cl and ^{27}Cl isotopes compared with their mirror levels in isobaric partners ^{26}F and ^{27}Ne. The vertical axis shows excitation energies E^*. The legends for levels give the spin-parity J^π and energies relative to the $1p$-emission threshold for the Cl chain members or the $1n$-emission threshold for their isobaric mirror partners. The given uncertainty of the states is due to variation of unknown charge radii of unstable sulfur daughter nuclei (see Fig. 12 in Ref. [1]).

the data, see Table II) demonstrate considerable deviations from the isotone expectation. These deviations have one major source—the Thomas-Ehrman shift (TES) effect—which is a well-established phenomenon and which is reliably described by the cluster model used in Ref. [1] and here.

On the basis of the developed S_p systematics for the chlorine isotopic chain, we can turn to the systematics studies of the argon isotopic chain. Following the approach of Ref. [1] we apply the systematics of odd-even staggering energies (OES):

$$2E_{\rm OES} = S_{2p}^{(A)} - 2S_p^{(A-1)} = 2S_p^{(A)} - S_{2p}^{(A)}$$

(see Fig. 4). For the chlorine isotopic chain beyond the dripline there is the trend of overbinding because of the TES. For the argon isotopic chain there should be a competition of two trends: (i) overbinding because of the TES (the Coulomb displacement energy decreases because of an increase of the valence orbital size) and (ii) underbinding due to $E_{\rm OES}$ reductions (the pairing energy decreases because of an increase of the valence orbital size). This effect has been already emphasized in Ref. [2]. Thus for the limiting estimates of the S_{2p} in the argon isotopic chain we use the upper and lower estimates of S_p shown in Fig. 5(a), which are then added to the full $2E_{\rm OES}$ value and multiplied by a factor of 1/2. The obtained results are shown in Fig. 5(b). The S_p and S_{2p} values predicted for Ar and Cl isotopic chains are also collected in Table II.

TABLE II. The separation energies S_p and S_{2p} for chlorine and argon isotopes with mass A located beyond the proton dripline. The theoretical values are in the columns "Theory", and the measured values are in the columns "Expt., [Ref]" with the respective references.

A	$S_p(^A\text{Cl})$ (MeV)		$S_{2p}(^A\text{Ar})$ (MeV)	
	Theory	Expt., [Ref]	Theory	Expt., [Ref]
31			− 0.08(15)	0.006(34), [1]
30	− 0.311(1)	− 0.48(2), [1]	− 2.43(17)	-2.45^{+5}_{-10}, [3]
29	− 1.75(1)	− 1.8(1), [2]	− 2.93(25)	− 5.50(18),[a] [1]
28	− 1.83(2)	− 1.60(8), [1]	− 6.90(35)	
27	− 4.14(7)		− 8.90(40)	
26	− 4.66(9)		− 11.3(8)	
26			− 11.7(3)[b]	
25	− 6.15(15)			

[a]Not clear whether this is a ground state or an excited state.
[b]This theoretical result is obtained with the three-body model (see Fig. 6).

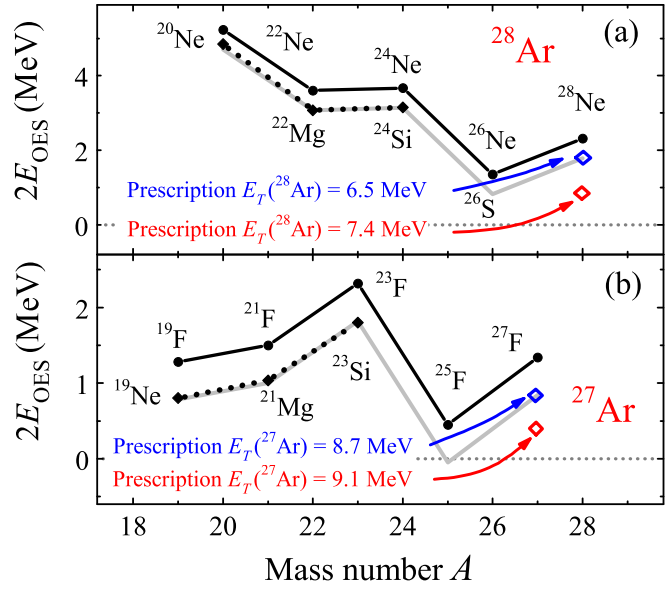

FIG. 4. Odd-even staggering energies $2E_{\rm OES} = S_{2N}^{(A)} - 2S_N^{(A-1)}$ for the isotones leading to ^{28}Ar (a) and ^{27}Ar (b) are shown by the dotted line. The OES energies for the mirror isobar are given by the solid line. The gray line is provided to guide the eye: this solid line is shifted down by constant values of about 0.5 MeV. The blue and red diamonds correspond to certain prescriptions of the two-proton decay energy E_T indicated in the legends and give odd-even staggering energies equal to either its systematic value or half of this value.

To conclude this section, the smaller than conventionally expected separation energies S_p and S_{2p} are predicted in this work for the chlorine and argon isotopes located far beyond the proton dripline. Such a general decrease should result in longer lifetimes of their ground and low-lying excited states, and consequently it may affect the limits of existence of nuclear structure beyond the proton dripline.

IV. LIMITS OF NUCLEAR-STRUCTURE EXISTENCE FOR CHLORINE AND ARGON ISOTOPIC CHAINS

One of the fundamental tasks of nuclear science studies is the determination of the limits of existence of individual states in nuclear systems. The half-life value can be chosen as a quantitative criterion of the nuclear-structure formation. Let us consider a system formed by a potential barrier and assume that to form a nuclear state there should be at least one reflection of the valence nucleon from the barrier. Then

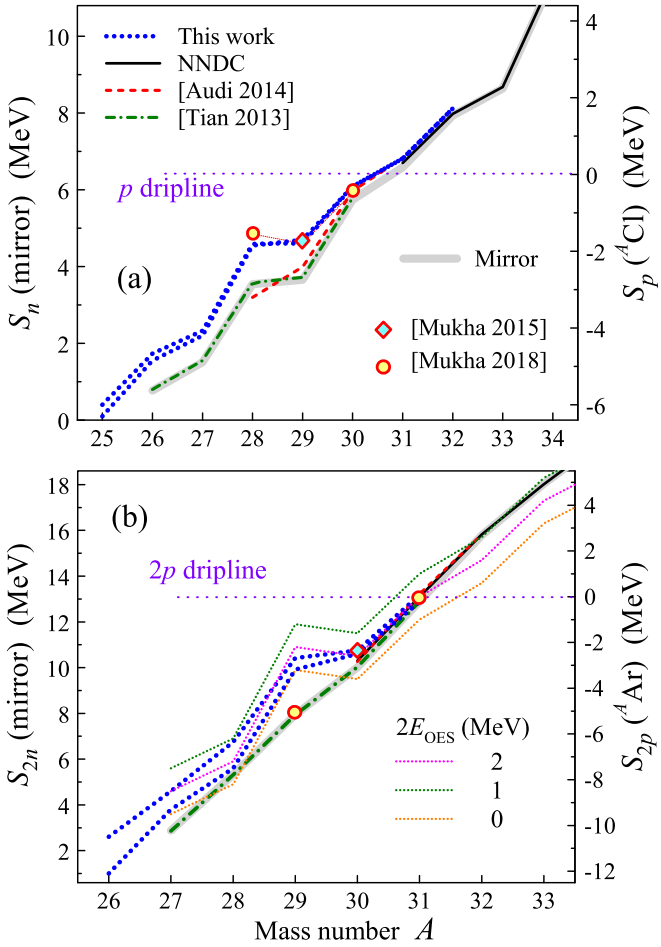

FIG. 5. Separation energies S_p for the chlorine isotopic chain (a) and S_{2p} for the argon one (b) from Ref. [5] are shown by the solid black lines. Separation energies S_n and S_{2n} for the mirror isotone chains are shown by the thick gray lines. The systematic evaluations from Refs. [6,7] are given by the red dashed and green dash-dotted lines. The results of this work and Ref. [1] based on the cluster model and E_{OES} systematics are shown by the blue dotted lines (there are two lines for upper and lower limiting estimates). The experimental values for ^{29}Cl and ^{30}Ar [2] are shown by the red diamonds, while the results of Ref. [1] are shown by the red circles.

the potentials of the $^A\mathrm{S} + p$ channel used in Ref. [1] and this work may help in estimations of such a limit for the chlorine isotopes by using the classical oscillation frequency

$$\nu = \left(2\int_{r_1}^{r_2}\frac{dr}{v(r)}\right)^{-1} = \left(\int_{r_1}^{r_2} dr\sqrt{\frac{2M}{E-V(r)}}\right)^{-1},$$

where r_1 and r_2 are two inner classical turning points. This oscillation frequency provides quite precise results (for sufficiently high barriers) when entering the expression for the quasiclassical estimate of width:

$$\Gamma = \nu P, \quad P = \int_{r_2}^{r_3} dr p(r),$$

where r_3 is outer classical turning point. For energies E varying from 0 to ~90% of the barrier height, the estimate

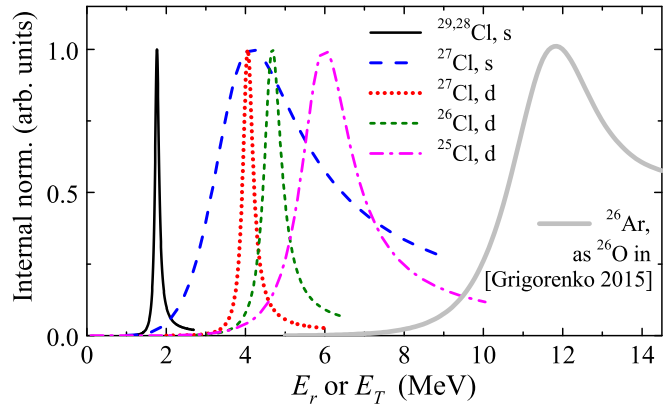

FIG. 6. Internal normalizations for the ground states of $^{25-29}$Cl isotopes as a function of the proton decay energy E_r. The gray solid curve shows the excitation spectrum of ^{26}Ar obtained in the three-body model as a function of the two-proton decay energy E_T. The same curve is given for both ^{28}Cl and ^{29}Cl, because the g.s. energies of these isotopes are predicted to be almost equal [1].

is $\nu \approx$ 1–3 MeV. Thus we can assume that the systems with widths exceeding 3–5 MeV have half-lives shorter than those needed for formation of the nuclear state. Such a system decays instantaneously, because, with a large probability, there will not be a single reflection from the potential barrier.

The width values of the chlorine isotopes can be estimated from the calculated excitation spectra that are illustrated in Fig. 6. For this purpose, we have used the internal normalization $N(E)$ of the two-body continuum wave function $\psi(kr)$,

$$N(E) = \int_0^{r_2} dr|\psi(kr)|^2,$$

as a measure of the resonance formation. This is done in contrast to conventional scattering phase shifts, which could not provide a firm signature of a resonance formation in the case of very broad nuclear states ($\Gamma \gtrsim 1$ MeV). One can see in Fig. 6 that s-wave states in chlorine isotopes become quite broad already in ^{27}Cl ($\Gamma \gtrsim 3$ MeV). However, the d-wave states remain reasonably narrow ($\Gamma \sim 1.5$ MeV) even in ^{25}Cl with its quite high decay energy $E_r \sim 6$ MeV.

In Fig. 7 we provide the *upper-limit* width estimates for the argon isotopes. They are performed in a "direct decay" R-matrix model from Ref. [8], where each proton is assumed to be in a resonant state of the core + p subsystem with the resonant energy E_{j_i}. The differential of the decay width is given by

$$\frac{d\Gamma_{j_1 j_2}(E_T)}{d\varepsilon} = \frac{E_T\langle V_3\rangle^2}{2\pi}\frac{\Gamma_{j_1}(\varepsilon E_T)}{\left(\varepsilon E_T - E_{j_1}\right)^2 + \Gamma_{j_1}^2(\varepsilon E_T)/4} \times \frac{\Gamma_{j_2}[(1-\varepsilon)E_T]}{\left[(1-\varepsilon)E_T - E_{j_2}\right]^2 + \Gamma_{j_2}^2[(1-\varepsilon)E_T]/4}, \quad (1)$$

where j_i is the angular momentum of a core + p_i subsystem. For the ground state decays $E_{j_1} = E_{j_2} = E_r$ and $\Gamma_{j_1} = \Gamma_{j_2} = \Gamma_r$. This model can be traced to the simplified Hamiltonian

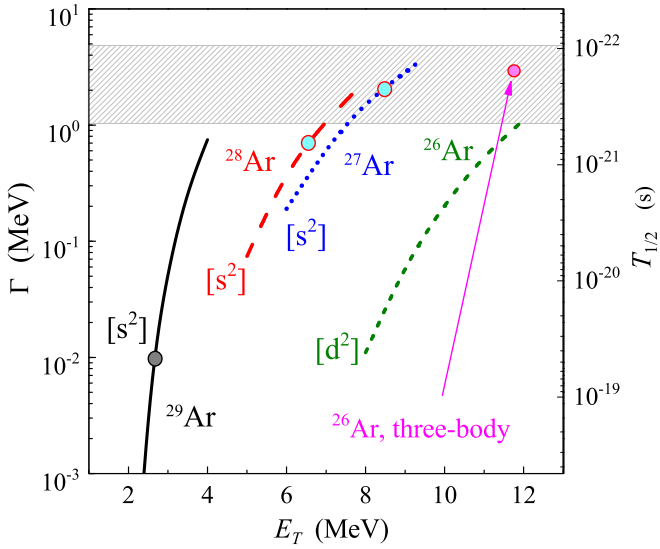

FIG. 7. Widths Γ and half-lives $T_{1/2}$ of the ^{29}Ar–^{26}Ar isotopes as functions of the decay energy estimated by a direct decay model. The obtained decay energy of ^{29}Ar [1] is indicated by the solid black circle. The energies predicted in this work are indicated by the red-cyan circles. The magenta arrow points to the $\{E_T, \Gamma\}$ position evaluated for the ^{26}Ar isotope by the three-body model (see Fig. 6). The hatched area indicates the half-life range where the nuclear structure begins to "dissolve."

of the three-body system in which the nucleons interact with the core, but not with each other. The model approximates the true three-body decay mechanism and also provides a smooth transition to the sequential decay regime [13,14]. The matrix element $\langle V_3 \rangle$ can be well approximated by

$$\langle V_3 \rangle^2 = D_3\{(E_T - E_{j_1} - E_{j_2})^2 + [\Gamma_{\rm ph}(E_T)]^2/4\},$$

where the parameter $D_3 \approx 1.0$–1.5 (see Ref. [14] for details), and $\Gamma_{\rm ph}(E_T)$ should provide smooth width behavior around $E_T \sim E_{j_1} + E_{j_2}$. The assumed R-matrix parameters for the widths,

$$\Gamma(E) = 2\,\frac{\theta^2}{2Mr_c^2}\,P_l(E, r_c, Z), \qquad (2)$$

in the chlorine isotopes are given in Table III. It was shown in Ref. [3] that the calculation has significant sensitivity to only the general decay parameters $\{E_T, E_r, \Gamma_r\}$.

TABLE III. The R-matrix parameters of the $^{A-2}$S + p channel adopted by the width estimates of ^{A}Ar isotopes: the angular momentum l, the channel radius $r_c = 1.2(A-1)^{1/3}$ in fm, the reduced width θ^2, the resonance energy E_r, and the corresponding width Γ_r in MeV.

A	l	r_c	θ^2	E_r	Γ_r
26	2	3.31	1.0	6.0	0.5
27	0	3.55	1.5	5.1	3.3
28	0	3.60	1.5	4.2	2.2
29	0	3.64	1.5	1.6	5.7×10^{-3}
31	0	3.73	1.5	0.5	5.3×10^{-6}
31	2	3.73	1.0	0.5	3.6×10^{-8}

For the width estimates presented in Fig. 7, we consider the initial structure and the decay of the argon isotopes via $[s^2]_0$ configurations with s-wave resonance parameters inherited from the two-body model calculations for the chlorine isotopic chain. Such an assumption guarantees the upper-limit width estimate (see discussions in Refs. [8,13,14]). However, this does not work for ^{26}Ar. The ^{25}Cl isotope which is a core + p subsystem of ^{26}Ar has a very "poor" spectrum with just one low-energy d-wave state. For that reason we make a $[d^2]_0$ estimate for ^{26}Ar decay. To cross-check it, we made three-body calculations of the excitation function in a full three-body model. It is known that, for $2N$ decays of higher orbital configurations, accounting for N-N final-state interaction may lead to a drastic decrease in the half-life [15]. The three-body calculations are completely analogous to the calculations of the ^{26}O g.s. in Ref. [16] with the added Coulomb interaction in the p-p and core-p channels. The corresponding excitation function is shown in Fig. 6. The obtained resonance energy $E_T \sim 11.7$ MeV is in good agreement with the systematic results of this work [see Fig. 5(b) and Table II]. The estimated width value $\Gamma \sim 3$ MeV is shown in Fig. 7.

To conclude this section, a number of relatively narrow states, which presumably can be interpreted in terms of nuclear structure, are predicted in the chlorine and argon isotopic chains down to ^{26}Ar and ^{25}Cl isotopes. These are located on the $N = 8$ shell closure and the lighter systems along these chains are not expected to exist. The population of such exotic systems is far beyond the reach of any modern experiment. However, we emphasize that there exists a rich, often not considered, research field far beyond the proton dripline that does not seem to be exhaustable in the observable future.

V. SYNERGY EFFECT IN THE EXPERT SETUP

The experimental setup used in Refs. [1–4] is a pilot version of the EXPERT project proposed for the physics program of the Super-FRS Experiment Collaboration of the FAIR facility (see Refs. [11,12]). The EXPERT setup will be located mainly in the middle of the Super-FRS fragment separator: the first part will produce and separate ions of interest, and the second part will measure momenta of heavy-ion decay products with high precision. The EXPERT setup is being tested at the FRS at GSI (Darmstadt). It consists of the following devices (see Fig. 1): (i) a charged-particle tracking system based on microstrip silicon detectors (μSSD) located downstream of the secondary target in the S2 middle focal plane of the FRS, (ii) an OTPC at the end of the FRS, and (iii) γ-ray detectors around the secondary target GADAST. An important part of the EXPERT initiative is (iv) the use of the second half of the FRS as a high-resolution spectrometer. This feature provides unique $\{A, Z\}$ identifications for a number of possible long-lived (i.e., with $T_{1/2} \gtrsim 100$ ns) heavy-ion reaction products and their implantation into the OTPC for radioactivity studies.

The instruments (i)–(iii) can be operated as independent devices and each of them has scientific value of their own. However, for studies of nuclear systems beyond the dripline, the elements of the EXPERT setup operated together provide

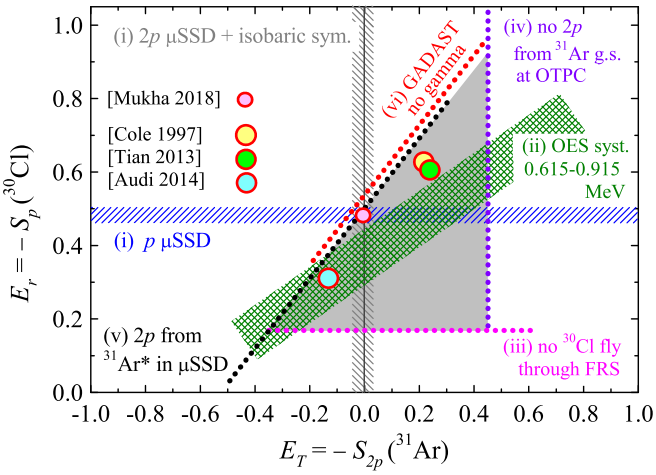

FIG. 8. The limitations on the correlated values of S_p in ^{30}Cl and S_{2p} in ^{31}Ar from different types of data and estimates (see text). The predictions of systematics studies [6,22] are shown by circles.

an important synergy effect that has not been discussed so far. Let us demonstrate such a synergy effect by example of the ^{30}Cl and ^{31}Ar g.s. studies.

Figure 8 shows the constraints that can be imposed on the ground-state energies of ^{30}Cl and ^{31}Ar connected with different types of measurements and theoretical considerations given below. They are partly based on the half-life estimates of these isotopes presented in Fig. 9. First, let us explain Fig. 9. The half-life of ^{30}Cl is calculated for the $^{29}\mathrm{S}+p$ s-wave decay by the R-matrix model [see Eq. (2)]. The half-life of ^{31}Ar ground and first-excited states are estimated by the R-matrix-type direct-decay three-body model [see Eq. (1), Table III, and the corresponding discussion]. The calculations are performed assuming the $[s^2]$ and $[sd]$ configurations in the $^{29}\mathrm{S}+p+p$ channel, respectively. For the ^{31}Ar first-excited state the $2p$-decay energy $E_T \sim 1$ MeV is expected, while for the ^{30}Cl g.s. the expectation is $E_r \sim 0.5$ MeV [1]. Therefore for this state the turnover from a true $2p$-decay mechanism to a sequential $2p$-decay mechanism is expected at $E_T \gtrsim E_r$. These decay modes are characterized by very different behavior of width as a function of energy. We have estimated three half-life curves for the ^{31}Ar first-excited state corresponding to the assumed ^{30}Cl g.s. energies of 0.4, 0.55, and 0.7 MeV, which are shown in Fig. 9 by the red dotted curves.

One should note that the widths of states are estimated for the fastest possible s-wave proton emission from ^{30}Cl as well as the fastest $[s^2]$-wave $2p$ decay from the ^{31}Ar g.s. We have also assumed that the first process in the decay of the ^{31}Ar excited state is the emission of the s-wave proton, which is a very conservative estimate because the ^{30}Cl g.s. has presumably an s-wave configuration. So, the more realistic half-life limitations could be even more stringent than those provided below.

Now we turn to a description of the obtained limits on the decay energies of ^{31}Ar and ^{30}Cl, which are illustrated in Fig. 8. There are in total six different limitations connected with observation or/and nonobservation of different states and decay channels in these systems.

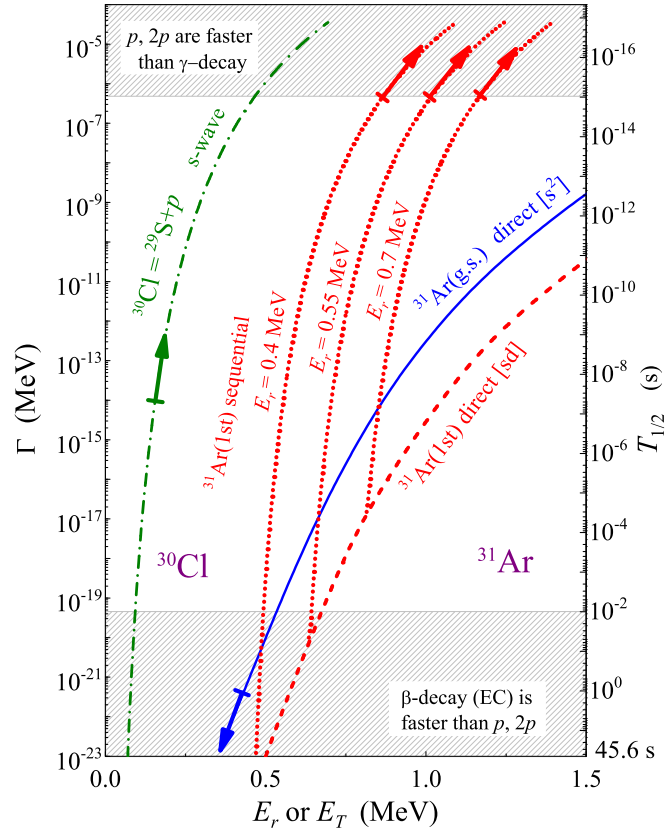

FIG. 9. Proton and two-proton decay widths Γ and half-lives $T_{1/2}$ of ^{30}Cl and ^{31}Ar as a function of decay energies E_r (for p emission) or E_T (for $2p$ emission). True $2p$ decay of the ^{31}Ar g.s. is shown by the solid blue curve. True $2p$ decay of the ^{31}Ar first-excited state is shown by the dashed red curve. Transition to sequential decay of the ^{31}Ar first-excited state is illustrated by the dotted red curves for different ^{30}Cl g.s. positions. The $1p$ decay of the ^{30}Cl g.s. (assuming s-wave emission) is shown by the green dash-dotted curve.

(i) The horizontal and vertical hatched bands correspond to the energies directly inferred from the measurements by the μSSD tracking system as discussed above in this work and in Ref. [1].

(ii) The diagonal hatched band is provided on the basis of systematics of the OES energies of Fig. 13(a) from Ref. [1]. We assume that isobaric symmetry for ^{31}Ar is a good assumption, giving $2E_{\mathrm{OES}} = 0.915$ MeV. In Fig. 8 we assume that some deviation from this value (-300 keV) is possible but not too much, and $2E_{\mathrm{OES}} = 0.615$ MeV is taken as the lower limit.

(iii) The ions of ^{30}Cl were not observed at the final focal plane of the FRS. This means that the half-life of ^{30}Cl is shorter than the time-of-flight (ToF) through the S2–S4 section of the FRS which is around 150 ns. We use the ToF value of 50 ns as the upper-limit estimate. This imposes the corresponding lower-limit estimate $E_r > 160$ keV (see the green arrow in Fig. 9 and the magenta horizontal dotted line in Fig. 8).

(iv) The ^{31}Ar isotopes were implanted into the OTPC to study β-delayed proton emission [23]. A nonobservation limit value is less than the obtained

branching ratio of $7(2) \times 10^{-4}$ for the β-delayed decay channel of ^{31}Ar. This means that the ^{31}Ar g.s. energy is $E_T < 0.4$ MeV (see the blue arrow in Fig. 9 and the vertical violet dotted line in Fig. 8). Otherwise, the prompt $2p$ emission from ^{31}Ar becomes faster than its β decay.

(v) The estimated half-live curves for $2p$ decay of the ^{31}Ar first-excited state are given in Fig. 9. It is clear that, if the partial half-life of ^{31}Ar with respect to $2p$ emission is longer than $\sim$1 fs, then the preferable decay branch for this state is γ deexcitation to the ground state. Since the $2p$ decay of the ^{31}Ar first-excited state is really observed, then the half-life limitations indicated by the red arrows in Fig. 9 infer synchronous limitations on both the proton decay energy E_r of the ^{30}Cl g.s. and the two-proton decay energy E_T of the ^{31}Ar first-excited state. The latter is transferred into E_T of the ^{31}Ar g.s. in Fig. 8 by subtracting 0.96 MeV as assumed from isobaric symmetry with ^{31}Al in Ref. [1] (inclined black dotted line). For example, let us consider the $E_r = 0.7$ MeV curve in Fig. 9. It provides the $E_T = 1.17$ MeV limit and thus leads to the black dotted line passing through point $\{0.21, 0.7\}$ in Fig. 8.

(vi) Analogous information could be inferred from nonobservation of γ rays from the γ decay of the ^{31}Ar first-excited state in GADAST (the inclined red line in Fig. 8). The statistics in the current experiment was not sufficient to make this information significant, but in a general case it could provide an additional cross-check of consistency for the different types of data.

All in all, the limitations shown in Fig. 8 lead together to a dramatic reduction of the area admissible for the correlated ^{30}Cl vs ^{31}Ar g.s. energies compared to the data provided by the μSSD tracking detectors of the EXPERT only. We should state here that the confidence in the results for ^{30}Cl and ^{31}Ar g.s. energies is strongly enforced by the synergy analysis presented here.

VI. SUMMARY

In this work we use the data [1] concerning the most remote from the proton dripline $^{30-28}$Cl and $^{31-29}$Ar isotopes, which allow for further advances in studying an unknown domain beyond the proton dripline. The main results of this work are the following.

(i) The systematic studies of the chlorine and argon isotopic chains beyond the proton dripline have been performed. Large Thomas-Ehrmann shifts were revealed for the ^{29}Cl and ^{30}Ar isotopes in Ref. [2], and here we report further increased values in the ^{28}Cl and ^{30}Cl isotopes. The predictions for the very remote from the dripline isotopes $^{25-27}$Cl and $^{26-28}$Ar are provided by the elaborated models. For these isotopes, the Thomas-Ehrmann effect becomes less important because (a) the isobaric mirror partners of these nuclides are located in proximity to the neutron dripline and (b) the ground states are d-wave states, which are less prone to modification by the Thomas-Ehrmann shift.

(ii) The obtained decay energies for the experimentally observed cases ($^{28-30}$Cl nuclides [1]) are considerably different (smaller) from the systematic trends available in the literature. The extrapolations to even lighter chlorine and argon isotopes also continue this trend. Smaller decay-energy systematics means "survival" of the nuclear structure for even more remote from the dripline particle-unstable systems. The limits of nuclear-structure existence for the proton-rich edge of chlorine and argon isotope chains are predicted to be in ^{26}Ar and ^{25}Cl.

(iii) An amazingly small $2p$-separation energy of 6(34) keV of the ^{31}Ar ground state reported in the preceding article [1] has been explored in addition by using the complementary data available in the setup and relevant theoretical speculations. The synergy effect of the measurements performed by different detectors of the EXPERT setup was demonstrated. It gives stronger support to the conclusions about the decays of ^{30}Cl and ^{31}Ar isotopes.

ACKNOWLEDGMENTS

This work was supported in part by the Hessian Ministry for Science and Art (HMWK) through the LOEWE funding scheme Helmholtz International Center for FAIR (HIC for FAIR); the Helmholtz Association (Grant No. IK-RU-002); the Russian Science Foundation (Grant No. 17-12-01367); the Polish National Science Center (Contract No. UMO-2015/17/B/ST2/00581); the Polish Ministry of Science and Higher Education (Grant No. 0079/DIA/2014/43, Grant Diamentowy); the Helmholtz- CAS Joint Research Group (Grant No. HCJRG-108); the Ministry of Education & Science, Spain (Contract No. FPA2016-77689-C2-1-R); the Ministry of Education, Youth and Sports, Czech Republic (Projects No. LTT17003 and No. LM2015049); and the Justus-Liebig-Universität Giessen (JLU) and the GSI under the JLU-GSI strategic Helmholtz partnership agreement. This work was carried out in the framework of the Super-FRS Experiment collaboration. This article is a part of the Ph.D. thesis of D. Kostyleva.

[1] I. Mukha *et al.*, Phys. Rev. C **98**, 064308 (2018).
[2] I. Mukha *et al.*, Phys. Rev. Lett. **115**, 202501 (2015).
[3] T. Golubkova, X.-D. Xu, L. Grigorenko, I. Mukha, C. Scheidenberger, and M. Zhukov, Phys. Lett. B **762**, 263 (2016).
[4] X.-D. Xu *et al.*, Phys. Rev. C **97**, 034305 (2018).
[5] National Nuclear Data Center, http://www.nndc.bnl.gov.
[6] G. Audi, M. Wang, A. Wapstra, F. K. M. MacCormick, and X. Xu, Nucl. Data Sheets **120**, 1 (2014), compilation $A = 1$–270, atomic masses, and other properties.
[7] J. Tian, N. Wang, C. Li, and J. Li, Phys. Rev. C **87**, 014313 (2013).

[8] M. Pfützner, M. Karny, L. V. Grigorenko, and K. Riisager, Rev. Mod. Phys. **84**, 567 (2012).
[9] P. G. Sharov, I. A. Egorova, and L. V. Grigorenko, Phys. Rev. C **90**, 024610 (2014).
[10] L. V. Grigorenko, N. K. Timofeyuk, and M. V. Zhukov, Eur. Phys. J. A **19**, 187 (2004).
[11] Technical Design Report of the EXPERT Setup for the Super-FRS Experiment Collaboration, http://edms.cern.ch/document/1865700.
[12] J. Aysto *et al.*, Nucl. Instrum. Methods Phys. Res., Sect. B **376**, 111 (2016).
[13] L. V. Grigorenko and M. V. Zhukov, Phys. Rev. C **76**, 014008 (2007).
[14] L. V. Grigorenko and M. V. Zhukov, Phys. Rev. C **76**, 014009 (2007).
[15] L. V. Grigorenko, I. G. Mukha, and M. V. Zhukov, Phys. Rev. Lett. **111**, 042501 (2013).
[16] L. V. Grigorenko and M. V. Zhukov, Phys. Rev. C **91**, 064617 (2015).
[17] J. B. Ehrman, Phys. Rev. **81**, 412 (1951).
[18] R. G. Thomas, Phys. Rev. **88**, 1109 (1952).
[19] C. R. Hoffman *et al.*, Phys. Rev. Lett. **100**, 152502 (2008).
[20] Y. Kondo *et al.*, Phys. Rev. Lett. **116**, 102503 (2016).
[21] M. D. Jones, K. Fossez, T. Baumann, P. A. DeYoung, J. E. Finck, N. Frank, A. N. Kuchera, N. Michel, W. Nazarewicz, J. Rotureau, J. K. Smith, S. L. Stephenson, K. Stiefel, M. Thoennessen, and R. G. T. Zegers, Phys. Rev. C **96**, 054322 (2017).
[22] B. J. Cole, Phys. Rev. C **54**, 1240 (1996).
[23] A. A. Lis *et al.*, Phys. Rev. C **91**, 064309 (2015).